Voltage-Clamp Studies on Uterine Smooth Muscle

NELS C. ANDERSON, Jr.

From the Departments of Obstetrics and Gynecology, and the Department of Physiology and Pharmacology, Duke University Medical Center, Durham, North Carolina 27706

ABSTRACT   These studies have developed and tested an experimental approach to the study of membrane ionic conductance mechanisms in strips of uterine smooth muscle. The experimental and theoretical basis for applying the double sucrose-gap technique is described along with the limitations of this system. Nonpropagating membrane action potentials were produced in response to depolarizing current pulses under current-clamp conditions. The stepwise change of membrane potential under voltage-clamp conditions resulted in a family of ionic currents with voltage- and time-dependent characteristics. In sodium-free solution the peak transient current decreased and its equilibrium potential shifted along the voltage axis toward a more negative internal potential. These studies indicate a sodium-dependent, regenerative excitation mechanism.

INTRODUCTION

In their now famous series of voltage-clamp experiments Hodgkin, Huxley, and Katz (1952) and Hodgkin and Huxley (1952 a, b, c, d) showed that the excitation process in the squid giant axon has its basis in time- and voltage-dependent ionic conductance changes. The regenerative mechanism producing the rising phase of the action potential was shown to be the result of a voltage-dependent increase in sodium conductance and repolarization due to inactivation of sodium conductance and a delayed increase in potassium conductance.

More recently voltage control techniques have been applied to skeletal (Adrian et al., 1968) and cardiac muscle (Reuter and Beeler, 1969; Rougier et al., 1968).

In smooth muscle, characterization of the passive electrical properties and testing of the ionic theory of excitation are complicated by a number of factors. From the anatomical point of view, small cell size and the complex interfiber geometry not only present severe technical problems but also provide the tissue with properties peculiar to interacting multicellular units.

A variety of evidence indicates that visceral or unitary (Bozler, 1941, 1948) smooth muscle is best characterized as an electrical syncytium (Tomita, 1966; Nagai and Prosser, 1963; Abe and Tomita, 1968; Barr et al., 1968). Resting

145

and action potential recording across many cell lengths in the single sucrose gap (Anderson, 1964; Marshall and Csapo, 1961; Kao, 1967) directly supports the concept of electrical coupling between uterine smooth muscle cells. The structural basis of intercellular coupling is probably the nexal junction as described by Dewey and Barr (1964) and Evans and Evans (1964). Bergman (1968) has also recently described the nexal junction in rat uterine smooth muscle.

The involvement of multicellular units in propagated activity is indicated by the evidence that with external current injection the spread of electrotonic currents covers many cell lengths (Abe and Tomita, 1968; Nagai and Prosser, 1963; Tomita, 1966). Furthermore, the equivalent space constant calculated from these data is more than a millimeter and, therefore, many cell lengths long. In addition, Abe and Tomita (1968) have suggested that the passive electrical properties of taenia coli can be expressed in terms of simple cable theory as applied to nerve and skeletal muscle (Hodgkin and Rushton, 1946).

These considerations suggest that, in response to externally injected current, there should be relatively uniform change in potential over a length of smooth muscle which is small relative to the calculated space constant. Thus the double sucrose-gap technique developed by Julian, Moore, and Goldman (1962) for lobster axons was used in the application of space-clamp and voltage-clamp conditions to strips of uterine smooth muscle.

The purpose of these studies was to develop and test an experimental approach to the study of membrane ionic conductance mechanisms in uterine smooth muscle. With the sucrose-gap voltage-clamp system the voltage- and time-dependence of the ionic excitation mechanisms has been demonstrated. Furthermore, changes in the transient current-voltage relation in sodium-free solution indicated a sodium-dependent excitation mechanism.

MATERIALS AND METHODS

Uterine Smooth Muscle Preparation

Strips of rat myometrium were used in all experiments. Because of the wide variations in uterine smooth muscle structure and function with stages of the estrous cycle and pregnancy, virgin rats, approximately 100 days old, were spayed and 1 wk later injected subcutaneously with 100 μg estradiol benzoate per day for 5 days. This procedure provided a well-defined preparation from an endocrine point of view as well as a tissue with extensive intercellular coupling (Bergman, 1968). Approximately 1 day after the last injection the rat was killed by cervical dislocation and the entire uterus dissected out and placed in normal Krebs solution. With the aid of a dissecting microscope and fine (No. 5) watchmaker forceps, strips of myometrium were dissected as described below.

One point of the watchmaker forceps was forced through the myometrium in the transverse direction. With the 100–500 μ wide strip held securely in the forceps, one end was cut loose and a strip of muscle obtained by carefully pulling in the longitudinal direction. Such strips were 1–3 cm long.

NODE TEST

SUCROSE — — SUCROSE

Vpool (K$_2$SO$_4$) — — Ipool (KREBS)
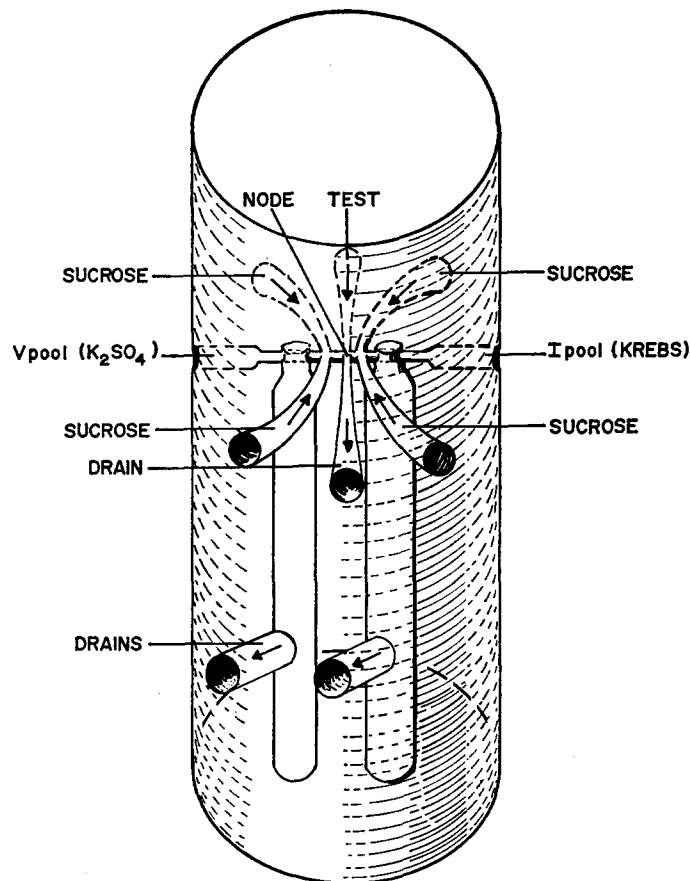
SUCROSE — — SUCROSE

DRAIN

DRAINS

Figure 1. The principles of operation of this chamber are the same as those presented by Julian et al. (1962). However, this chamber differs in that the critical plumbing is not machined but rather molded from Epoxy and fitted into a large outer Plexiglass block which contains control valves and electrodes. V_{pool} (voltage pool) and I_{pool} (current pool) connect to the side pools of the outer chamber which in turn connect to the electrometer and external stimulator, respectively (see Fig. 2). Test solution flows over the node area of the muscle from a central pool in the outer chamber. In the diagram of the molded central core arrows indicate the direction of solution flow. Node refers to the approximately 100 μ wide space between the sucrose gaps. Node width and stability are controlled by adjusting sucrose and test solution flow rates by means of valves in the outer chamber. Test solution flowing over the node area also represents the central or ground pool, since this solution is in direct contact with the electrode connected to the summing junction of the current amplifier (see Fig. 2).

Sucrose-gap Chamber

The sucrose-gap chamber may be considered as three separate pools, with the two end pools separated from the middle pool by high resistance sucrose gaps (Fig. 1). The muscle strip is mounted in the chamber so that the ends are in the side pools and the sucrose streams form insulating cuffs around the muscle strip, thus isolating a
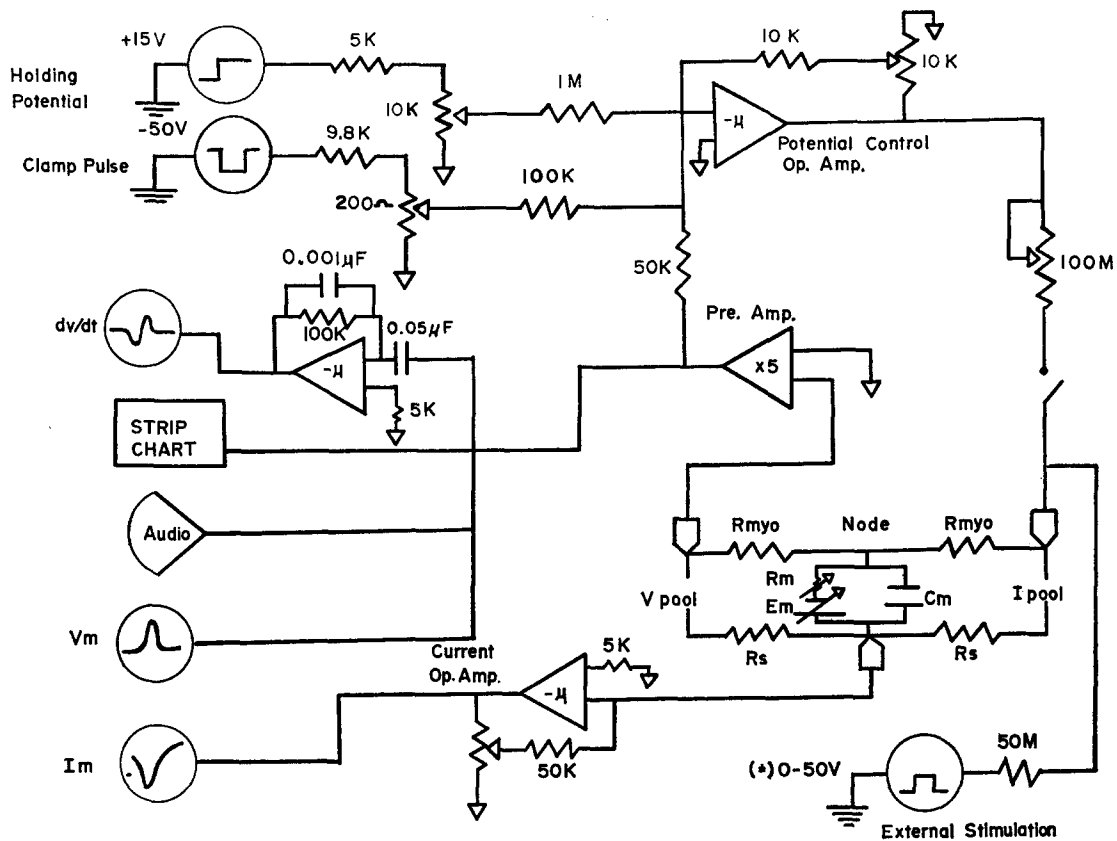
FIGURE 2. Current-clamp and voltage-clamp circuit diagram. The electrical equivalent of a space-clamped smooth muscle strip in the sucrose-gap chamber is included in the lower right portion of the circuit diagram. Sucrose (R_s) and myoplasmic (R_{myo}) resistances are indicated on either side of the central node area. The node membrane unit represents the short length of muscle strip ($\simeq 100$ μ) isolated between the sucrose gaps. With an open switch in the feedback loop the system is in current-clamp configuration. Under these conditions positive current pulses injected into the right-hand pool (I pool) induce depolarization of the node membrane.

Node membrane potentials were recorded across the left-hand sucrose gap, i.e. between the left-hand pool (V pool) and ground (central pool), with a high input impedance electrometer. The central pool electrode was connected directly to the summing junction of the current operational amplifier and thus maintained at virtual ground potential.

The output of the preamplifier was sent to: (a) a strip chart recorder, (b) an audio monitor, (c) a differentiating operational amplifier, (d) Tektronix 564 storage oscilloscope, and (e) to the summing junction of the control amplifier.

The transition from current clamp to voltage clamp involves closing the switch in the feedback loop and decreasing the large (100 Mohm) resistance between the output of the control amplifier and the I pool electrode. Components of the voltage control system include the node membrane, preamplifier, and control amplifier. With the node membrane in the feedback loop the control amplifier injects or withdraws current necessary

small patch of membrane or artificial "node" in the middle pool. When viewed under a dissecting microscope, the liquid junctions of sucrose and test solutions were clearly seen to define the node area.

Solutions for the three pools and the sucrose solutions flowed by gravity from reservoir bottles into stainless steel coils in a constant temperature water bath mounted close to the chamber. From the bath the solutions dripped into Plexiglass dropper bottles which functioned to electrically isolate the solutions entering the chamber from the bath. All solutions were maintained at 32°C ± 1°C. Needle valves built into the channels from the dropper bottles to the chamber allowed adjustment of flow rates and hence control of the node area.

Potential and Current Measurement

Operational considerations of the sucrose-gap technique follow directly from the above discussion of chamber design. From left to right (Fig. 1) the pools are designated: voltage or V pool; ground or center pool; and current or I pool, respectively. Large, low resistance (less than 200 ohms) Ag-AgCl electrodes were connected to all three pools through Krebs-agar bridges.

The membrane potential was measured with a high input impedance preamplifier connected between the V pool and ground. The resting membrane potential was established by exposing the V pool end of the muscle strip to isotonic K_2SO_4 (125.1 mM). Since the center pool was maintained at virtual ground potential, the electrometer effectively measured an injury potential between the "inside" of the muscle strip in the V pool and the "outside" at the node or center pool. External stimulating current was provided by pulses from a Tektronix 161 pulse generator through a 50 megohm isolation resistor.

The voltage-clamp and current-clamp circuit diagram is presented in Fig. 2. Fundamental components of the voltage-clamp control system include: (a) a high input impedance electrometer, (b) a control amplifier (high gain, inverting, operational amplifier), and (c) holding and clamp pulse command signals. With the feedback loop closed (switch shown on the right of Fig. 2, closed) and the large resistance in series with the output of the control amplifier shorted, the circuit is in voltage-clamp configuration. Membrane current was measured with an operational amplifier as described by Moore (1959). The fact that the summing junction of an inverting operational amplifier is held near ground potential (virtual ground) provides these amplifiers with effectively zero input impedance. This property makes the operational amplifier approach an ideal current-measuring device. The center pool electrode was connected directly to the summing point of the current amplifier whose output voltage was proportional to the membrane current. The gain of the current amplifier was variable; however, it was routinely set for unity gain.

---

to make *Vm* match the command signals. The current output of the control amplifier thus matches that flowing across the membrane. Current was measured with an operational amplifier connected directly to the central pool electrode.

Membrane voltage and current were displayed on a dual beam oscilloscope and photographed on 35 mm film.

With an open switch in the feedback loop (see Fig. 2), the system is in the current-clamp mode. Under these conditions positive current pulses injected into the I pool produced depolarization of the node membrane and at "threshold" potential triggered membrane action potentials (Fig. 4). The output of the electrometer was also sent to a differentiating operational amplifier for measurement of maximum rates of rise and fall of action potentials, and also to an audio monitor and strip chart recorder which provided a continuous record of the experiment. Photographic records of membrane voltage and current were obtained from a Tektronix 564 storage oscilloscope. More recently these measurements have been recorded directly on magnetic tape. With data in this form leakage current correction and current-voltage plots of voltage-clamp data were obtained from Linc 8 computer analysis.

Testing, calibration, and balancing of the entire system were greatly facilitated by the use of an idealized membrane model. This consisted of a capacitor (0.05 μF) shunted by a parallel resistor (100 kohms) with 15 kohm resistors on the I pool and V pool sides of the model representing access or myoplasmic resistance. The rise time of voltage clamp on this model was 400 μsec.

Solutions

(*a*) Normal Krebs: NaCl 118.46 mM, KCl 4.74 mM, KH$_2$PO$_4$ 1.18 mM, MgSO$_4$ 1.18 mM, CaCl$_2$ 2.54 mM, NaHCO$_3$ 24.87 mM. Normal Krebs and test solutions flowing over the node area contained 11.5 mM glucose and were oxygenated with 95 % O$_2$-5 % CO$_2$. (*b*) Sodium-free solution: Sodium-free Krebs solution was prepared by replacing NaCl with an equal molar amount of Tris chloride, and NaHCO$_3$ with KHCO$_3$. KCl and KH$_2$PO$_4$ were omitted. Stock Tris-Cl was prepared from 1 M solution of Sigma Trizma base which was titrated to pH 7.4 with 10 N HCl. (*c*) Isotonic K$_2$SO$_4$ and KCl: 125.1 mM K$_2$SO$_4$; 150 mM KCl. (*d*) Sucrose: Isotonic sucrose (10 % w/v) was made up in deionized water and passed through a Crystalab Model CL-5 Deminizer (Crystalab, Hartford, Conn.). The conductivity of this solution was 0.6 μmho or less. When the conductivity was greater than 0.6 μmho, the ion exchange cartridge was replaced.

EXPERIMENTAL LIMITATIONS

Resting Membrane Potential

The accuracy of potential measurements in the sucrose-gap system is determined by two factors: (*a*) myoplasmic and intercellular bridge resistance, which is taken as "myoplasmic resistance;" and (*b*) the ability of sucrose to prevent short-circuiting between the voltage pool end of the muscle strip and the membrane in the area of the node.

Clearly in the case of single giant axons the simple geometry facilitates replacement of extracellular solutions with sucrose. In strips of smooth muscle, however, the situation is quite different. One is confronted on the one hand with slow outward diffusion of extracellular ions from deep within the bundle and on the other hand with continual replacement of extracellular ions

through active pumping mechanisms and nonspecific ion leakage. A further complication is the increase in myoplasmic resistance with prolonged exposure to sucrose. Sucrose-gap resistance determined in the absence of a muscle strip was 20-50 Mohms.

In view of these considerations, resting membrane potential measurements were defined as the steady-state membrane voltage recorded upon exposure of the V pool end of the muscle strip to isotonic K_2SO_4. These potentials ranged from -40 to -70 mv.

Membrane Area

In order to express ionic currents in terms of current densities (mamp/cm^2) it is necessary to have an accurate measure of total active membrane area. Because of the complex, multicellular geometry of the muscle strip there is no simple direct means of estimating total membrane area during an experiment. Therefore, in the present series of experiments, membrane currents are expressed in terms of absolute units of current (microamperes).

Series Resistance and Uniformity of Potential Control

The potential induced by current injection under space-clamp conditions (i.e. when the node width is 100 μ or less) is developed across the node membrane resistance and any resistance in series with the membrane to ground. In this system the series resistance has two components. One consists of solution and electrode resistance between the outside of the muscle strip and the summing point of the current amplifier. The second is "cleft" or extracellular space resistance from the inner fiber membranes to the outside of the muscle strip.

By definition, under voltage clamp, "the potential difference across the membrane capacitance shall have a known and constant value during the time and over the area of membrane in which the current flow is measured" (Cole and Moore, 1960). The membrane potential time course and shape observed during voltage-clamp pulses satisfy this criterion and thus the circuit performance is quite satisfactory (Fig. 6). However, from the above considerations of series resistance, the potential of membrane deep in the muscle strip differs from the measured value when current flows. Thus while the membrane potential of peripheral smooth muscle fibers may be controlled within 400 μsec under voltage-clamp conditions, as is indicated by the Vm record, the potential across fiber membranes deeper in the strip may be changing over a longer period of time. Sommer and Johnson (1968) have calculated the effect of cleft resistance on voltage control in cardiac muscle under these experimental conditions. This analysis clearly indicates a graded voltage response of inner fiber membranes as a function of cleft resistance. To minimize these problems it is obviously desirable to work with very small strips and to keep the external series resistance (solution and ground electrode resistance) as low as possible.

Another consideration in securing uniformity of potential control is apparent when one compares the axial current electrode system (Hodgkin et al., 1952) with the double sucrose-gap arrangement (Julian et al., 1962). With an axial electrode the axoplasmic resistance is "short-circuited," while in the double sucrose-gap system myoplasmic resistance is unchanged. When the membrane resistance is high and the node width narrow relative to the tissue space constant, the effect of this component in producing a longitudinal potential gradient with current flow is minimized. However, under voltage-clamp conditions when the membrane potential is pulsed to a value which activates membrane conductances, a further consideration appears; with the fall in membrane resistance the tissue space constant shrinks to smaller values allowing steeper longitudinal potential gradients when current is forced into one end of the node by feedback from the control amplifier. Therefore, although current is injected or withdrawn by the control amplifier, forcing Vm to match the command signals, the uniformity of potential over the node membrane is determined by the width of the node and relative myoplasmic and membrane resistances.

In view of these considerations it is apparent that quantitative and kinetic analyses of smooth muscle voltage-clamp data are limited. However, qualitative analysis of the ionic components of the excitation process as well as the testing of the effects of hormones and drugs on these parameters is feasible and justified.

RESULTS

Current Clamp

Within the first few minutes after mounting the muscle strip in the chamber, spontaneous bursts of action potentials were often observed. This activity was associated with contraction of the muscle strip beyond the node area. However, spontaneous action potential activity was readily abolished when the V pool end of the muscle was exposed to isotonic K_2SO_4 and positive current pulses were injected into the I pool. Under these conditions all regenerative activity originated from the node membrane. Furthermore, when viewed under a dissecting microscope, the muscle in the node area was not observed to "twitch" or move in response to current injection even though large regenerative action potentials were triggered. Thus, the boundaries of the length of muscle in the node area were not continuously changing as a result of action potential activity.

Responses of the node membrane potential to hyperpolarizing and depolarizing current pulses are illustrated in Fig. 3. Hyperpolarizing current pulses resulted in a linear current-voltage relation. The time course of these induced potentials was roughly exponential having a time constant of 80 msec. Depolarizing pulses which lowered the membrane potential to threshold triggered local membrane action potentials in the node.
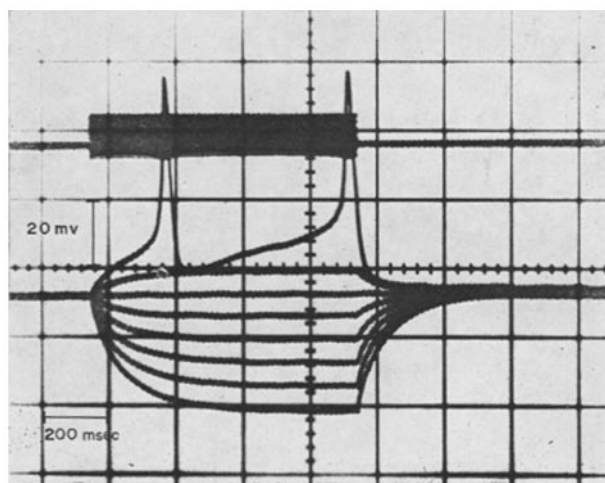
Figure 3. Node membrane potential responses (lower tracings) to depolarizing and hyperpolarizing current pulses (upper tracings). Current steps were 0.2×10^{-6} amp.
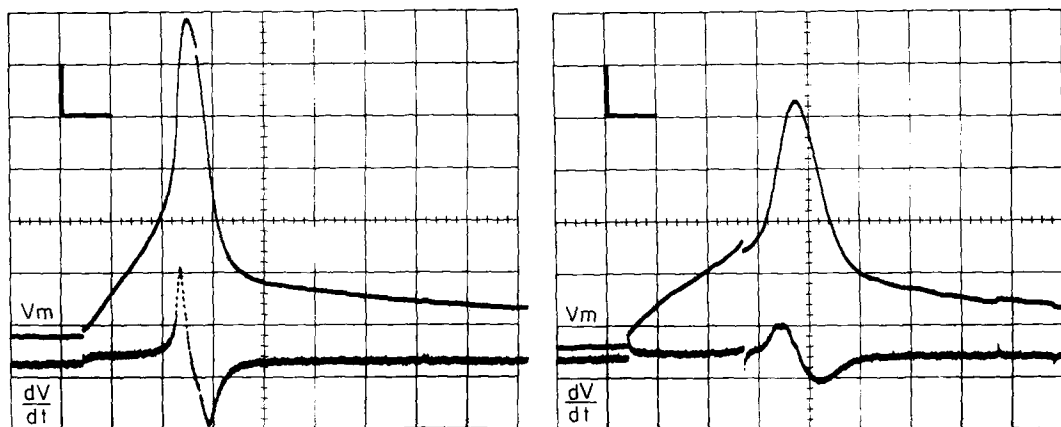

Figure 4 *a*   Figure 4 *b*

Figure 4. Local membrane action potentials. Since both action potentials (a and b) are from the same node area in response to a constant strength current pulse, differences in action potential waveform probably reflect the complex multifiber structure of the node membrane and intrinsic variations in fiber excitability. Calibrations, Vm, 10 mv/cm and 20 msec/cm on oscilloscope grid; dV/dt, 25 v/sec per cm on oscilloscope grid.

Variable responses to a constant current pulse (Fig. 4) raise questions related to threshold potential, graded vs. all-or-none-responses and interpretation of compound action potential waveform, time course, and amplitude. Fig. 4 *a* represents a synchronous excitation response of the node membrane. Deviations from this waveform (Fig. 4 *b*) without changing the stimulus strength or duration may be explained in terms of intrinsic variations in fiber
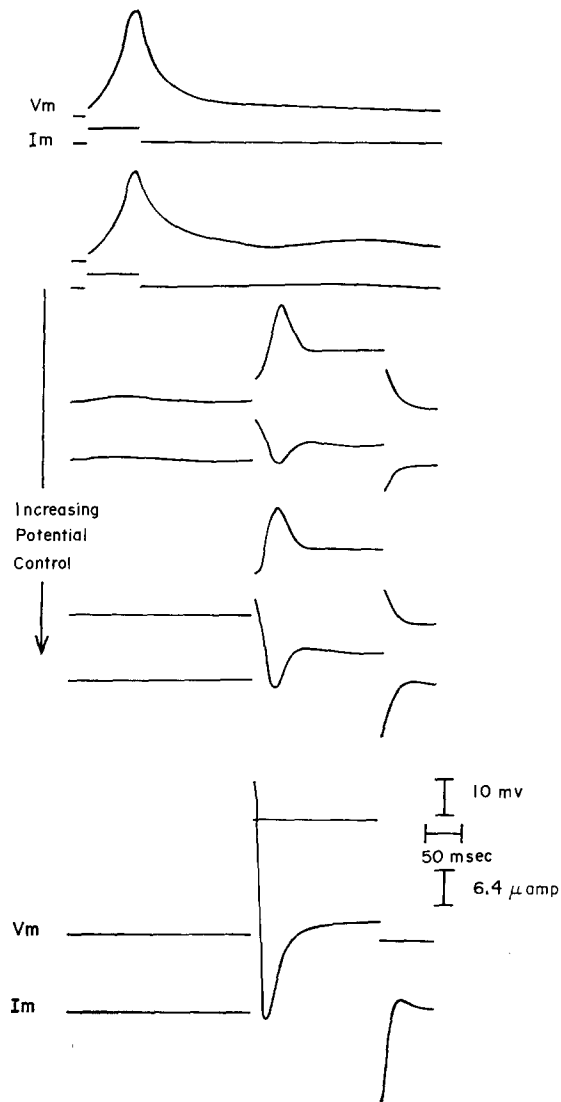
FIGURE 5.   The transition from current clamp (upper *Im* and *Vm* tracings) to voltage clamp (lower *Im* and *Vm* tracings). Intermediate stages of voltage control demonstrate the condition in which the membrane potential does not follow the rectangular voltage-clamp command signal.

excitability. This interpretation is supported by the observation that with supramaximal stimulation the action potential waveform stabilized. Thus at threshold the population of fibers or percentage of node membrane being activated may be relatively small and variable. With increasing stimulus strength there is a net increase in node membrane activated which is reflected in increased dV/dt and spike amplitude and in decreased delay in activation.

Decreased spike height associated with increased delay in activation may also reflect partial inactivation of the regenerative mechanism.

Intracellular recording from node fibers is necessary to determine whether single fibers undergo graded or all-or-none responses under these conditions. To minimize variation in action potentials, supramaximal stimulation was used routinely.

Voltage Clamp

A. CLOSING THE FEEDBACK LOOP

With the demonstration of a stable resting potential and membrane action potentials, conditions were set for applying voltage clamp to the muscle strip.
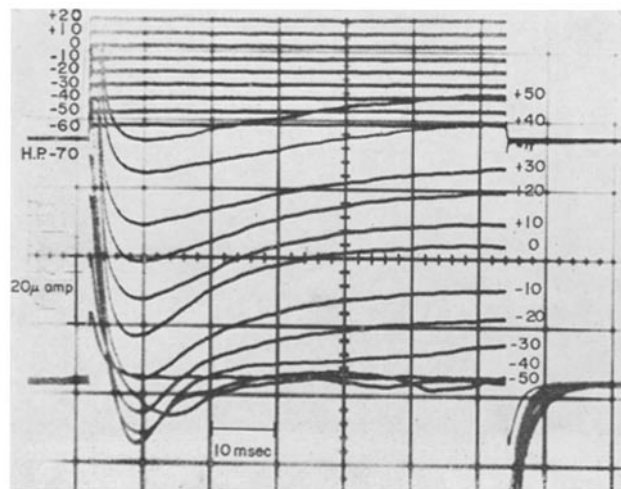

FIGURE 6. Family of membrane currents produced in response to stepwise change of membrane potential from the holding potential (H.P.) of −70 mv under voltage-clamp conditions.

As the series resistance in the feedback loop was gradually reduced (see Fig. 2), the membrane potential went through graded stages of control (Fig. 5). With the series resistance shorted, placing the node membrane directly in the feedback loop, any tendency for ionic currents to change the charge on the membrane capacitance during a clamp pulse was compensated for by the control amplifier injecting or withdrawing current necessary to make V_m match the command signals. The output of the control amplifier thus follows membrane ionic conductance changes.

B. DEPOLARIZING POTENTIAL STEPS UNDER VOLTAGE-CLAMP CONDITIONS

Stepwise change of the membrane potential under voltage-clamp conditions resulted in a family of ionic currents with voltage- and time-dependent char-

acteristics (Fig. 6). Voltage control as judged from the rise time and time course of the voltage records was satisfactory. Components of the current records shown in Fig. 6 include: (a) an initial capacitive and time-dependent leakage current, (b) transient inward current, and (c) a delayed steady-state outward current.
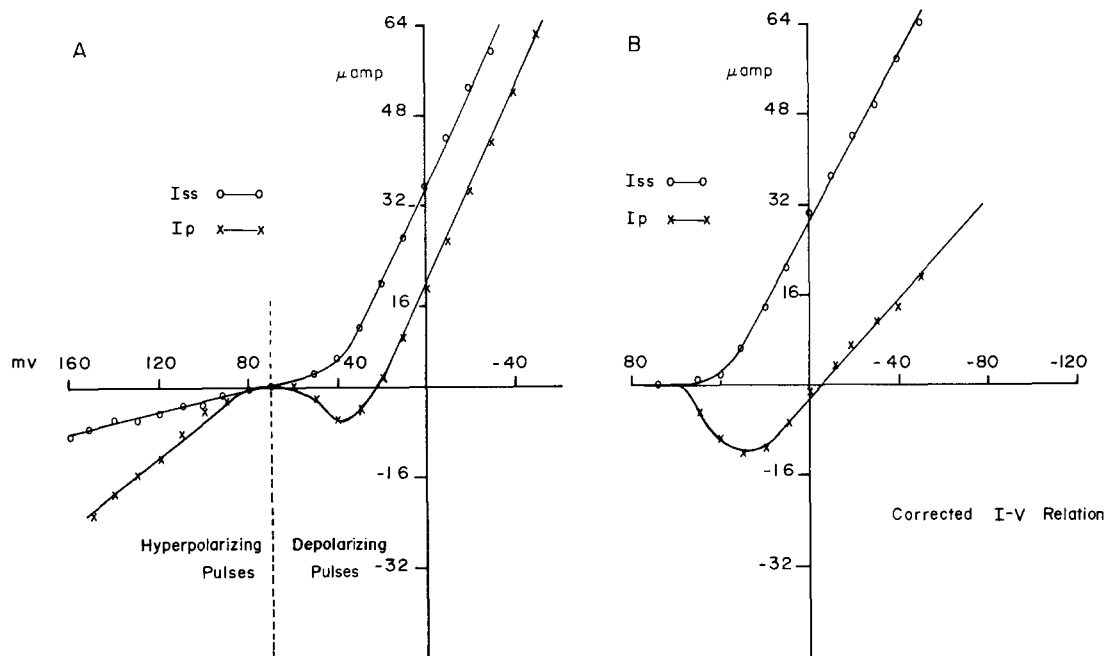

Figure 7. Current-voltage (I-V) relations under voltage-clamp conditions. A, currents in the depolarizing direction are plotted as peak transient (I_p) and steady-state (Iss) currents. Currents generated in response to hyperpolarizing voltage-clamp pulses are plotted as steady state and "I_p" where I_p is taken as that value of Im corresponding in time to the peak transient current during an equal displacement of the membrane potential in the depolarizing direction, B, current-voltage relation after correction for leakage currents. Net active or leakage corrected current-voltage relations were obtained by subtracting currents from depolarizing and hyperpolarizing voltage-clamp pulses. Note the negative slope of the transient current-voltage relation and the positive equilibrium potential.

C. CORRECTION FOR LEAKAGE CURRENT

Leakage current correction for analysis of net active membrane current was based on the observation that the time-dependent and steady-state leakage currents are linear functions of hyperpolarizing pulses (Fig. 7). Furthermore, membrane currents produced by small displacements of the membrane potential to either side of the holding potential were symmetrical (Fig. 9). On this basis it was assumed that leakage current was linear for all values of membrane

potential. If this assumption is true, leakage correction by scaling current from a small hyperpolarizing pulse should yield the same current-voltage relation as subtracting currents from opposite polarity pulses (pattern difference leakage correction). Fig. 8 illustrates the two different systems of leakage correction. Current-voltage relations (Fig. 8 X) were obtained by summing currents from equal but opposite polarity clamp pulses. Current-voltage relations (Fig. 8, open triangles) were obtained by scaling current from a 10 mv hyperpolarizing pulse to all depolarizing pulse currents. The two systems yield the same current-voltage plots. It has also been demonstrated that
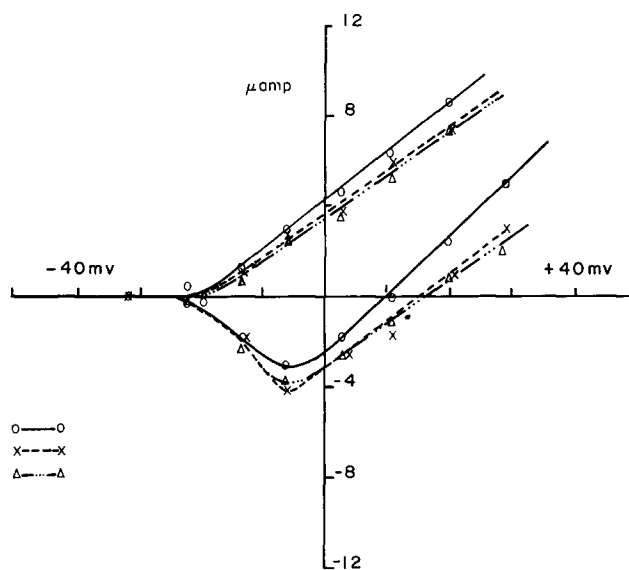

FIGURE 8. Current-voltage relation as corrected for leakage by two different methods: open circles, uncorrected; X, pattern difference leakage correction; open triangles, scaled pulse leakage correction (see text for further explanation).

pulsing the membrane potential in the hyperpolarizing direction beyond approximately −150 mv often leads to very nonlinear responses probably representing breakdown of the membrane.

D. CURRENT-VOLTAGE RELATIONS UNDER VOLTAGE-CLAMP CONDITIONS

During the voltage-clamp run the membrane was either alternately depolarized and hyperpolarized as in Fig. 9 or, based on the scaled leakage correction system, a family of depolarizing pulses was followed by a single 10 mv hyperpolarizing pulse. A family of currents obtained from a series of depolarizing and hyperpolarizing potential steps is presented in Fig. 9 a. The current-voltage relations before and after correction for leakage current
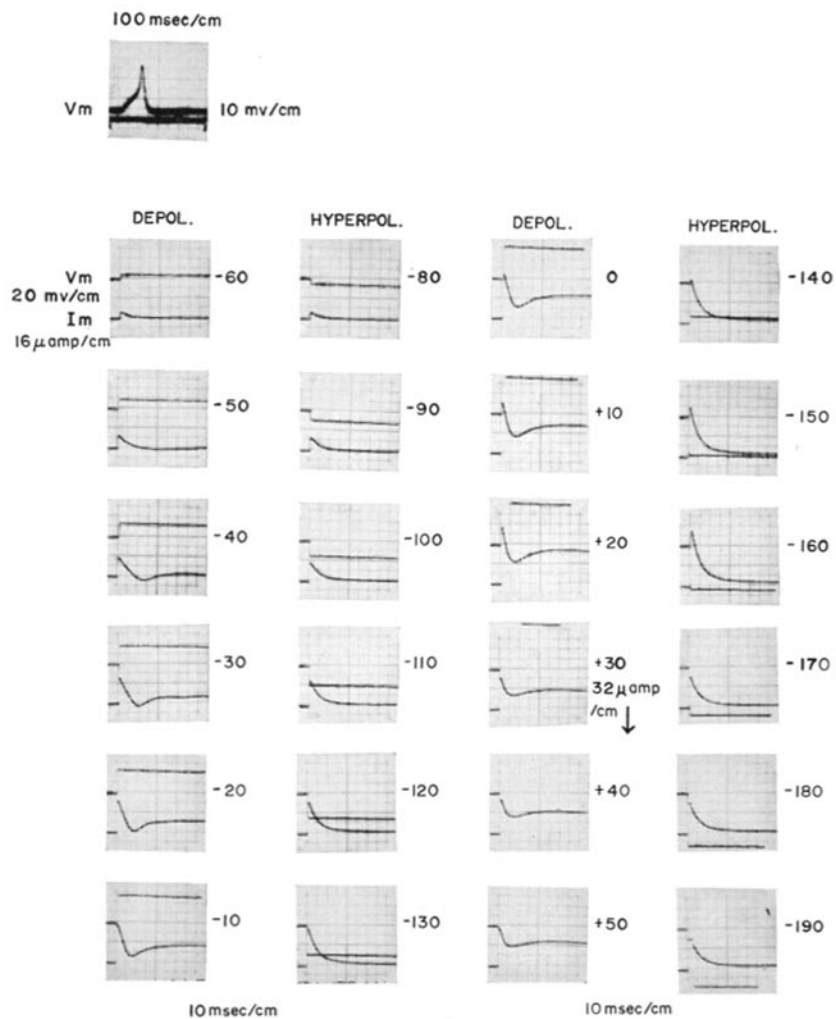
FIGURE 9 a

FIGURE 9 a and b.   Action potentials in the upper left-hand corner of both figures were obtained from the node prior to applying voltage clamp. FIG. 9 a. Membrane currents from a series of depolarizing and hyperpolarizing voltage-clamp pulses. Note that currents from hyperpolarizing clamp pulses have been inverted. This was done to facilitate data analysis. Hyperpolarizing current-voltage relations were linear. FIG. 9 b. Membrane currents, associated with depolarizing steps to −60 and −50 mv absolute membrane potential, demonstrated multiple peak transient currents. Voltage control, as judged by the voltage record, was good. It is suggested that this type of current record reflects the multicellular composition of the node membrane. With larger voltage steps the current record assumes a simpler waveform with capacitive, transient inward and steady-state outward components. The waveform of the membrane action potential associated with this node area also suggests a complex excitation mechanism. Note that the current and voltage calibrations refer to centimeter divisions on the oscilloscope grid.

are presented in Fig. 7 A and B, respectively. Leakage correction resulted in shifting the transient current equilibrium potential from the negative to the positive voltage axis. The negative transient current equilibrium potential predicts that the node action potential would not overshoot. While this
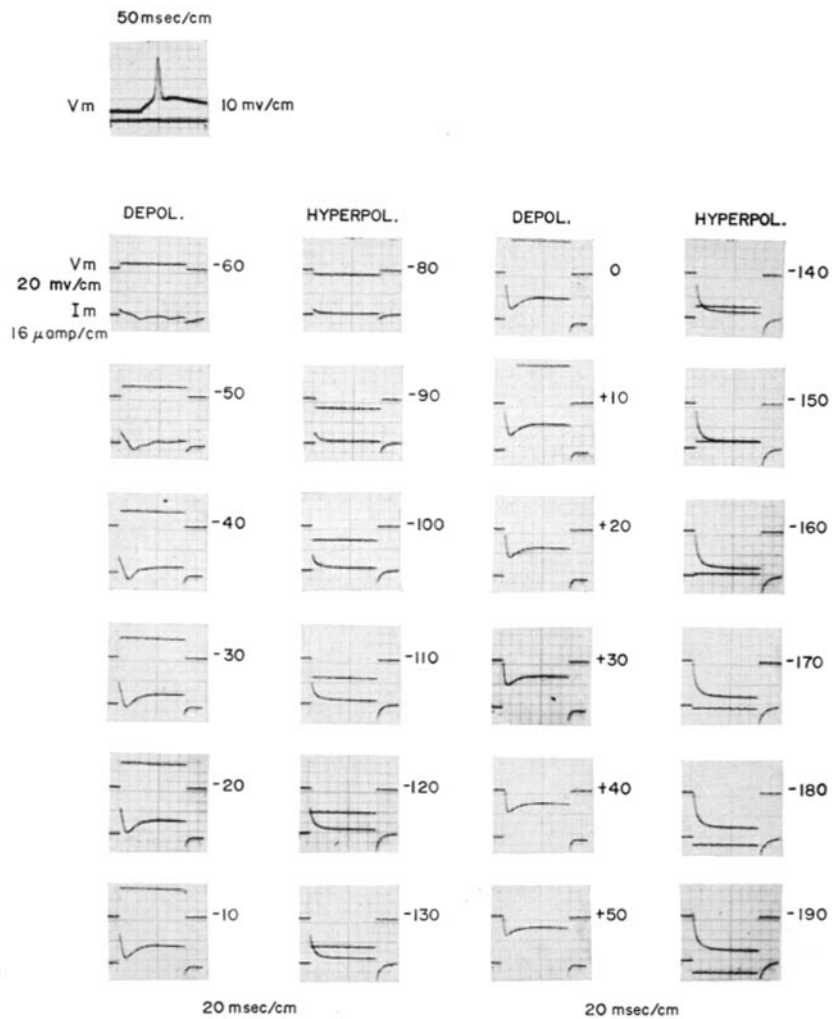

FIGURE 9 *b*

relationship generally holds true, the accuracy of predicting spike height from the uncorrected transient current equilibrium potential was only within 10–15 mv.

In Fig. 9 *b* membrane currents, associated with depolarizing steps to −60 and −50 mv absolute membrane potential, demonstrate multiple peak transient currents. Voltage control, however, as judged by the voltage record

was good. It is suggested that this type of current record reflects both the multicellular response as well as intrinsic variations in excitability of smooth muscle fibers, particularly at threshold potentials. With larger depolarizing voltage steps the current record assumes a simple waveform with capacitive, active transient and steady-state components. The waveform of the membrane action potential associated with this node area (upper left of Fig. 9 b) also suggests a complex excitation mechanism.
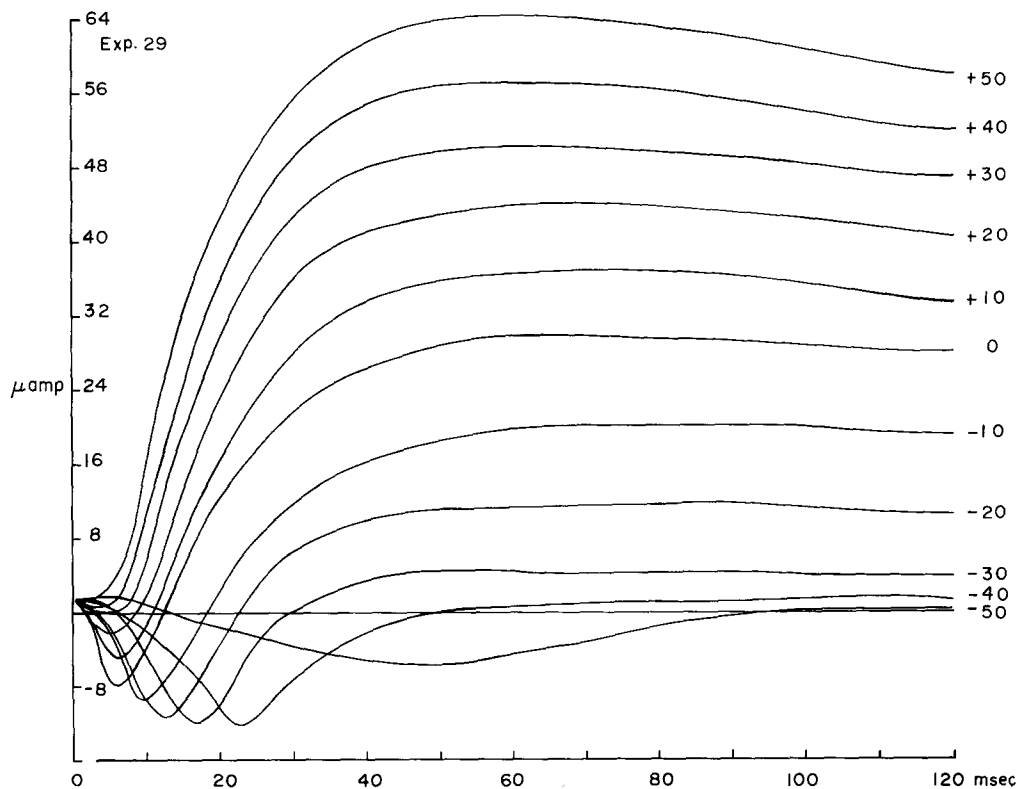

FIGURE 10. Family of membrane currents after correction for leakage currents under voltage-clamp conditions. Note that at +30 mv absolute membrane potential the transient current starts off horizontally indicating the transient current equilibrium potential.

Figs. 7 and 8 show that the transient current-voltage relation is a smooth, graded, and continuous function of membrane potential. Furthermore, the "N"-shaped, transient current-voltage relation indicates a region of negative resistance, associated with net inward current.

The family of leakage-corrected currents illustrated in Fig. 10 shows that at the transient current equilibrium potential, about +30 mv, the membrane current starts off horizontally and with time turns into an outward current component.

EXP 29

μamp   64

N.K. Before   x——x   56

Na+ Free,1.5 min •——•

Na+ Free,11.5 min o——o   48

N.K. After 7.0 min ▲——▲

N.K. After 11.5 min △——△   40

32

16

8

mv   -60   +60
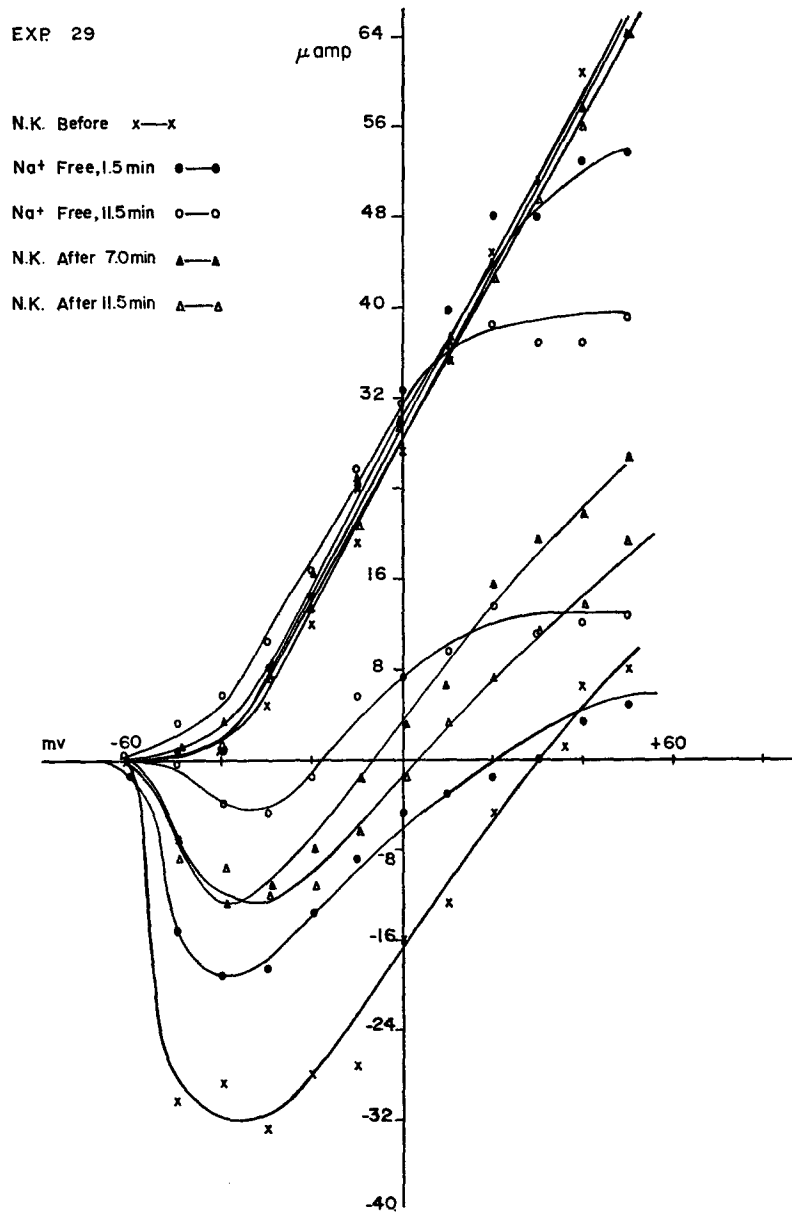
-8

-16

-24

-32

-40

FIGURE 11. Current-voltage relations under voltage-clamp conditions before, during, and after exposure to sodium-free medium. Note the decrease in the transient current and the shift in the transient current equilibrium potential along the voltage axis toward a lower internal potential.

Na+-Free Experiments

Current-voltage relations from one of five experiments are illustrated in Fig. 11. In normal Krebs before Na-free test solution the peak transient current (I_p) was 32 μamp and E_t (transient current equilibrium potential) +30 mv. After 1.5 min exposure to Na-free Krebs I_p had fallen to 10 μamp and E_t had shifted along the voltage axis toward a lower internal potential (+20 mv). After 11.5 min I_p was 4 μamp and E_t had moved to −18 mv. 7 min after returning to normal Krebs the transient current had again increased and E_t shifted along the voltage axis toward the value before exposure to Na-free solution. Recovery from exposure to Na-free solution was incomplete.

In these experiments the substitution of $KHCO_3$ for $NaHCO_3$ resulted in increased extracellular potassium concentration. In other sodium-free experiments in which Tris was substituted for $NaHCO_3$ and the potassium concentration maintained constant, the transient current again decreased and the current-voltage relation shifted along the voltage axis toward a lower internal potential. Recovery in normal Krebs likewise resulted in increased peak inward current and a shift of E_t back to near the original value.

DISCUSSION

The assumptions for applying voltage-control to uterine smooth muscle are as follows: (*a*) space-clamp or current-clamp conditions are established when the length of muscle isolated between the sucrose streams is 100 μ or less, (*b*) all membrane in the node area functions as a synchronous unit, and (*c*) voltage control is possible when these conditions are satisfied. For reasons outlined in the section on experimental limitations these assumptions are probably only approximated experimentally. Operational definitions of the experimental system based on measurable parameters have therefore been adopted. A stable resting membrane potential, uniform membrane action potentials together with node width 100 μ or less served as criteria for applying voltage clamp. The time course and shape of membrane voltage during voltage-clamp pulses served as the basis for judging the degree of voltage control. When the membrane potential deviated from the rectangular command pulse, as during intermediate stages of voltage control illustrated in Fig. 5, voltage control was judged inadequate for experimentation.

The current-voltage relation under current-clamp conditions was shown to be linear for hyperpolarizing current pulses and with depolarizing pulses demonstrated a discontinuous relation at threshold potential with the generation of a membrane action potential.

The observed variations of spike height and delay in activation complicate interpretation of compound action potential waveform, amplitude, and time course. Tomita (1966) and Casteels and Kuriyama (1965) have suggested

that the response of smooth muscle to current injection is in part dependent on rhythmic fluctuations in the excitability of smooth muscle membranes. The variable response to threshold stimulation in the present studies also supports the concept of intrinsic control of fiber excitability. Furthermore, in view of the multicellular composition of the node membrane, graded fiber excitability very likely leads to graded synchronization of fiber activity, particularly at threshold strength stimulation, resulting in variations in the compound action potential waveform, amplitude, and time course (also see Kao, 1967).

The large capacitive leakage current component, following a step depolarization, masks the onset of the active transient inward current. The system of "leakage" correction for extracting net active membrane current was based on the observation that the current-voltage relation for hyperpolarizing pulses is linear and, furthermore, that currents from small depolarizing and hyperpolarizing pulses are symmetrical. Based on these findings it was assumed that leakage current was linear for all values of membrane potential and that the difference in currents resulting from pulses of opposite polarity represented active membrane current. Reversal of current flow at the transient current equilibrium potential was also masked by the initial capacitive leakage current and became evident only upon leakage correction.

The magnitude of the shift of the transient current-voltage relation along the voltage axis, after leakage correction, emphasizes the effect of leakage current on uterine smooth muscle excitation. It appears that leakage current may significantly limit the ability of active transient inward current to depolarize the membrane.

Kao and Nishiyama (1964) and Casteels and Kuriyama (1965) have calculated the sodium equilibrium potential to be $+23$ mv in estrogen-dominated uterine smooth muscle. Under voltage-clamp conditions in sodium-free solution the equilibrium potential shifted along the voltage axis from an average E_t of $+17$ mv (five experiments) toward a more negative internal potential. These data support earlier observations on the sodium dependency of uterine smooth muscle action potentials (Kleinhaus and Kao, 1966; Marshall, 1963; Goto and Woodbury, 1958). Sodium flux studies by Kao et al. (1961) and Kao and Zakim (1962) are also in agreement with the observed effect of sodium deficiency under voltage-clamp conditions.

The insensitivity of taenia coli action potentials to tetrodotoxin (Kuriyama et al., 1966) and Na^+-deficient solutions (Holman, 1957, 1958; Bülbring and Kuriyama, 1963) together with the calcium dependency of excitation (Kuriyama et al., 1966; Bülbring and Kuriyama, 1963) has suggested that Ca^{++} ions may, in addition to affecting Na^+ activation as has been demonstrated in nerve (Frankenhaeuser and Hodgkin, 1957), actively carry

transient inward current in the generation of action potentials. Daniel and Singh (1958) have also reported that the myometrium is capable of generating action potentials in Na^+-deficient solution. Kao (1967) has recently suggested that many of these different experimental results may be accounted for in terms of incomplete depletion of Na^+ from the complex extracellular space. Sommer and Johnson (1968) have proposed a similar explanation of persistent inward current in sodium-free media as reported by Düdel et al. (1966) in cardiac muscle. The role of calcium and its relation to sodium in uterine smooth muscle excitation remain to be studied under voltage-clamp conditions.

REFERENCES

ABE, Y., and T. TOMITA. 1968. Cable properties of smooth muscle. *J. Physiol. (London).* **196**:87.

ADRIAN, R. H., W. K. CHANDLER, and A. L. HODGKIN. 1968. Voltage clamp experiments in striated muscle fibers. *J. Gen. Physiol.* **51** (5, Pt. 2):188.

ANDERSON, N. 1964. Relationship of relaxin to other hormones of pregnancy in the regulation of uterine activity. Ph.D. Thesis, Purdue University.

ANDERSON, N., and J. W. MOORE. 1968. Voltage-clamp of uterine smooth muscle. *Fed. Proc.* **27**:704. (Abstr.)

BARR, L., W. BERGER, and M. M. DEWEY. 1968. Electrical transmission at the nexus between smooth muscle cells. *J. Gen. Pyysiol.* **51**:347.

BERGMAN, R. A. 1968. Uterine smooth muscle fibers in castrate and estrogen-treated rats. *J. Cell Biol.* **36**:639.

BOZLER, E. 1941. Influence of estrone on electrical characteristics and motility of uterine muscle. *Endocrinology.* **29**:225.

BOZLER, E. 1948. Conduction automaticity and tonus of visceral muscles. *Experientia.* **4**:213.

BÜLBRING, E., and H. KURIYAMA. 1963. Effects of changes in the external sodium and calcium concentrations on spontaneous electrical activity in smooth muscle of guinea-pig taenia coli. *J. Physiol. (London).* **166**:29.

CASTEELS, R., and H. KURIYAMA. 1965. Membrane potential and ionic content in pregnant and non-pregnant rat myometrium. *J. Physiol. (London).* **177**:263.

COLE, K. S., and J. W. MOORE. 1960. Ionic current measurements in the squid giant axon membrane. *J. Gen. Physiol.* **44**:123.

DANIEL, E. E., and H. SINGH. 1958. The electrical properties of the smooth muscle cell membrane. *Can. J. Biochem. Physiol.* **36**:959.

DEWEY, M. M., and L. BARR. 1964. A study of the structure and distribution of the nexus. *J. Cell Biol.* **23**:553.

DÜDEL, J., K. PEPER, R. RUDEL, and W. TRAUTWEIN. 1966. Excitatory membrane current in heart muscle (Purkinje fibers). *Pfluegers Arch. gesamte Physiol. Menschen Tiere.* **292**:255.

EVANS, D. H. L., and E. M. EVANS. 1964. The membrane relationships of smooth muscles: an electron microscope study. *J. Anat.* **98**:37.

FRANKENHAEUSER, B., and A. L. HODGKIN. 1957. The action of calcium on the electrical properties of squid axons. *J. Physiol. (London).* **137**:218.

GOTO, M., and J. W. WOODBURY. 1958. Effects of stretch and NaCl on transmembrane potentials and tension of pregnant rat uterus. *Fed. Proc.* **17**:58.

HODGKIN, A. L., and A. F. HUXLEY. 1952 *a.* Currents carried by sodium and potassium ions through the membrane of the giant axon of *Loligo. J. Physiol. (London).* **116**:449.

HODGKIN, A. L., and A. F. HUXLEY. 1952 *b.* The components of membrane conductance in the giant axon of *Loligo. J. Physiol. (London).* **116**:473.

HODGKIN, A. L., and A. F. HUXLEY. 1952 *c.* The dual effect of membrane potential on sodium conductance in the giant axon of *Loligo. J. Physiol. (London).* **116**:497.

HODGKIN, A. L., and A. F. HUXLEY. 1952 *d.* A quantitative description of membrane current and its application to conduction and excitation in nerve. *J. Physiol. (London).* **117**:500.

HODGKIN, A. L., A. F. HUXLEY, and B. KATZ. 1952. Measurement of current-voltage relations in the membrane of the giant axon of *Loligo. J. Physiol. (London).* **116**:424.

HODGKIN, A. L., and W. A. H. RUSHTON. 1946. The electrical constants of a crustacean nerve fiber. *Proc. Roy. Soc. Ser. B. Biol. Sci.* **133**:444.

HOLMAN, M. E. 1957. The effect of changes in sodium chloride concentration on the smooth muscle of the guinea-pig taenia coli. *J. Physiol. (London).* **136**:569.

HOLMAN, M. E. 1958. Membrane potentials recorded with high-resistance microelectrodes and the effects of changes in ionic environment on the electrical and mechanical activity of the smooth muscle of the taenia coli of the guinea-pig. *J. Physiol. (London).* **141**:464.

JULIAN, F. J., J. W. MOORE, and D. E. GOLDMAN. 1962. Current-voltage relations in the lobster giant axon membrane under voltage clamp conditions. *J. Gen. Physiol.* **45**:1217.

KAO, C. Y. 1967. Ionic basis of electrical activity in uterine smooth muscle. *In* Cellular Biology of the Uterus. Ralph M. Wynn, editor. Appleton-Century-Crofts Division Meredith Publishing Co., New York. P. 386.

KAO, C. Y., and A. NISHIYAMA. 1964. Ovarian hormones and resting potentials of uterine smooth muscle. *Amer. J. Physiol.* **207**:793.

KAO, C. Y., and D. ZAKIM. 1962. Sodium fluxes in uterine smooth muscle. *J. Gen. Physiol.* **45**:606A.

KAO, C. Y., D. ZAKIM, and F. BRONNER. 1961. Sodium influx and excitation in uterine smooth muscle. *Nature (London).* **192**:1189.

KLEINHAUS, A. L., and C. Y. KAO. 1966. Bioelectric actions of oxytocin. *Fed. Proc.* **25**:354.

KURIYAMA, H., T. OSA, and N. TOIDA. 1966. Effect of tetrodotoxin on smooth muscle cells of the guinea-pig taenia coli. *Brit. J. Pharmacol. Chemother.* **27**:366.

MARSHALL, J. M. 1963. Behavior of uterine muscle in na-deficient solutions; effects of oxytocin. *Amer. J. Physiol.* **204**:732.

MARSHALL, J., and A. I. CSAPO.1961. Hormonal and ionic influences on the membrane activity of uterine smooth muscle cells. *Endocrinology* **68**:1026.

MOORE, J. W. 1959. Electronic control of some active bioelectric membranes. *Proc. IEEE (inst. elec. Electron. Eng.)* **47**:1869.

NAGAI, T., and C. L. PROSSER. 1963. Electrical parameters of smooth muscle cells. *Amer. J. Physiol.* **204**:915.

REUTER, H., and G. W. BEELER. 1969. Sodium current in ventricular myocardial fibers. *Science.* **163**:397.

ROUGIER, O., G. VASSORT, and R. STÄMPFLI. 1968. Voltage clamp experiments on frog atrial heart muscle fibers with the sucrose gap technique. *Pfluegers Arch. gesamte Physiol. Menschen Tiere.* **301**:91.

SOMMER, J. R., and E. A. JOHNSON. 1968. Cardiac muscle, a comparative study of purkinje fibers and ventricular fibers. *J. Cell Biol.* **36**:497.

TOMITA, T. 1966. Electrical responses of smooth muscle to external stimulation in hypertonic solution. *J. Physiol. (London).* **183**:450.